Microchim Acta (2014) 181:1505–1512
DOI 10.1007/s00604-014-1193-x

ORIGINAL PAPER

Electrochemical immunoassay for the prostate specific antigen using ceria mesoporous nanospheres

Juan Peng · Ying-Di Zhu · Xing-Hua Li · Li-Ping Jiang · E. S. Abdel-Halim · Jun-Jie Zhu

Received: 23 October 2013 / Accepted: 29 January 2014 / Published online: 2 March 2014

Abstract We report on a sensitive electrochemical immunoassay for the prostate specific antigen (PSA). An immunoelectrode was fabricated by coating a glassy carbon electrode with multiwalled carbon nanotubes, poly(dimethyldiallylammonium chloride), CeO_2 and PSA antibody (in this order) using the layer-by-layer method. The immunosensor is then placed in a sample solution containing PSA and o-phenylenediamine (OPD). It is found that the CeO_2 nanoparticles facilitate the electrochemical oxidation of OPD, and this produces a signal for electrochemical detection of PSA that depends on the concentration of PSA. There is a linear relationship between the decrease in current and the concentration of PSA in the 0.01 to 1,000 pg mL^{-1} concentration range, and the detection limit is 4 fg mL^{-1}. The assay was successfully applied to the detection of PSA in serum samples. This new differential pulse voltammetric immunoassay is sensitive and acceptably precise, and the fabrication of the electrode is well reproducible.

Keywords Ceria · Electrochemical immunoassay · Catalysis · Prostate specific antigen

J. Peng · Y.-D. Zhu · X.-H. Li · L.-P. Jiang (✉) · J.-J. Zhu
State Key Laboratory of Analytical Chemistry for Life Science, School of Chemistry and Chemical Engineering, Nanjing University, Nanjing 210093, People's Republic of China
e-mail: jianglp@nju.edu.cn

J. Peng
School of Chemistry and Chemical Engineering, Ningxia University, Yinchuan 750021, People's Republic of China

E. S. Abdel-Halim
Petrochemical Research Chair, Department of Chemistry, College of Science, King Saud University, Riyadh 11451P.O. Box 2455, Kingdom of Saudi Arabia

Introduction

The detection of biomarkers plays a crucial role in basic medical researches as well as in clinical diagnostics [1, 2]. Immunoassay based protocol employing antibody-antigen interaction is one of the most important analytical techniques in the quantitative detection of biomarkers due to the highly specific molecular recognition of immunoreaction [3]. Because of the increasing need of in-time control of various diseases, the development of sensitive, rapid and low cost immunoassays has become a great challenge. In comparison with other immunological methods such as fluorescence [4], chemiluminescence [5], surface-plasmon resonance[6], or quartz crystal microbalance [7, 8], electrochemical immunoassay [9] has attracted considerable interest for its intrinsic advantages such as good portability, low cost, and high sensitivity. Therefore, different electrochemical immunosensors [10], particularly amperometric immunosensors [11], have been developed and extensively applied to the determination of biomarkers.

The emergence of nanomaterials has opened new opportunities for electrochemical immunosensors [12]. Some particular nanomaterials, such as gold and quantum-dot nanoparticles, have already been widely used due to their good biocompatibility [13, 14]. Recently, nanoscale materials with unique catalytic activities have attracted great interest because of their multiple applications in energy storage, chemical synthesis, and biomedical applications [15–17].

Ceria (CeO_2) is a useful promoter and an important component for three-way catalysts because of its unique redox properties, strong oxygen storage, and release capability via facile conversion between Ce^{3+} and Ce^{4+} oxidation states [18–20]. Researchers have discovered that the catalytic performance of CeO_2 has been greatly influenced by the structural properties, such as surface area, naked crustal planes, and surface states [21–23]. CeO_2 mesoporous spheres have been

of increasing interest in catalysis for their unique structural properties, such as high surface area, special interfaces, uniform size distribution, and well-defined pore technology. The penetrable shells allow the diffusion of chemical reagents toward the inside of the structure, and the high surface area and the pore channels are helpful in the adsorption. Recently, it is reported that nanosized ceria show pH dependent oxidase activity, which can quickly oxidize a series of organic substrates without any oxidizing agent [24]. Meanwhile, a colorimetric assay has been developed based on cerium oxide as an oxidase-mimetric agent [25]. CeO_2 nanoparticles have also been used for the construction of electrochemical hydrogen peroxide biosensor [26, 27]. However, to the best of our knowledge, the catalytic application of CeO_2 mesoporous spheres in electrochemical immunoassay has not been addressed yet extensively. The catalytic activity of ceria mesoporous spheres in aqueous media makes them a powerful tool for a wide range of potential applications in bioassay and biological areas.

Herein, a novel electrochemical immunoassay was designed for sensitive detection of prostate specific antigen (PSA). A three dimensional (3D) architecture was fabricated by combining multiwalled carbon nanotubes (MWCNTs) and CeO_2 mesoporous spheres using the layer-by-layer method. Owing to the good stability of CeO_2 mesoporous spheres and excellent conductivity of MWCNTs, the 3D architecture not only provided a highly suitable microenvironment for effective antibody immobilization, but also made the immobilized antibodies hold high stability and bioactivity. The CeO_2 nanoparticles showed excellent catalytic property toward the electrochemical oxidation of o-phenylenediamine (OPD), which could produce a sensitive signal for electrochemical detection of PSA. The procedure of the immunoassay was shown in Scheme 1. The immunoassay showed a high sensitivity and a wide linear range for rapid detection of PSA. This strategy provided a useful tool for sensitive detection of PSA in serum samples.

Experimental

Reagents

Prostate specific antigen (PSA) and PSA antibody were purchased from Shanghai Linc-Bio Science Co. LTD (http://www.linc-bio.net/main.asp). *Poly*(dimethyldiallylammonium chloride) (PDDA, MW = 10 000–20 000), 3-mercaptopropionic acid (MPA), bovine serum albumin (BSA), 1-ethyl-3-(3-dimethylaminopropyl) carbodiimide hydrochloride (EDC), N-hydroxysuccinimide (NHS), and tween-20 were obtained from Aldrich Chemical Co. All of the other chemicals were of analytical grade. O-phenylenediamine (OPD) is a highly cancerogenic compound and its use is prohibited in some countries. Doubly distilled water was used throughout the experiments. The clinical serum samples were from Nanjing Gulou Hospital.

Synthesis of ceria mesoporous nanospheres

Ceria mesoporous nanospheres were synthesized according to the reported methods [28]. In a typical synthesis, 1.0 g of $Ce(NO_3)_3 \cdot 6H_2O$ was dissolved in 1 mL of deionized water. Then, 1 mL of C_2H_5COOH and 30 mL of glycol were added with stirring to form a uniform solution. The mixed solution was sealed and heated at 180 °C for 200 min to get the products.

Fabrication of immunosensing interface

A glass carbon electrode (GCE) with diameter of 3 mm was successively polished to a mirror by using 0.3 and 0.05 μm alumina slurry followed by rinsing thoroughly with water. After successive sonication in 1: 1 nitric acid/water, acetone, and doubly distilled water, the electrode was rinsed with doubly distilled water and allowed to dry at room temperature. As shown in Scheme 1, first, 5 μL of 1.0 mg mL^{-1} MWCNTs solution was first dropped on the pretreated GCE and dried, and then immersed in a 500 μL PDDA (0.2 mg mL^{-1} in 0.1 M NaCl) solution for 30 min. After rinsing with water, the electrode was immersed into a solution of CeO_2 dispersion (0.5 mg mL^{-1}). After dried and rinsing, the electrode was immersed in a mixture solution of EDC (100 μL, 20 mg mL^{-1}) and NHS (100 μL, 10 mg mL^{-1}) for 30 min. Then, the above electrode was immersed in an aqueous solution of PSA antibody for 2 h for immobilization. Finally, the

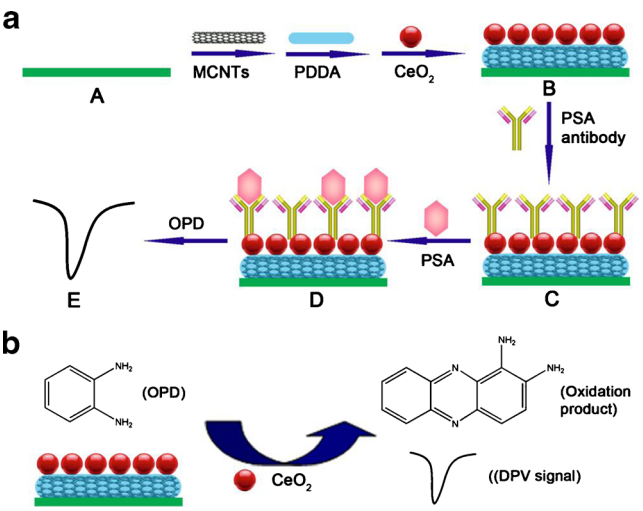

Scheme 1 **a** Schematic illustration of the procedure of the immunoassay: (**A**) Glassy carbon electrode (GCE); (**B**) Layer-by-layer assembly; (**C**) Immobilization of PSA antibodies; (**D**) PSA antibody-antigen immunoreaction; (**E**) Electrochemical detection of PSA antigen. **b** Electrochemical oxidation of OPD based on CeO_2 catalytic property

BSA solution was used to block the residual active sites. The immunoelectrode obtained was stored at 4 °C when not in use.

Immunoassay procedure

The above immunoelectrode was immersed into a solution of PSA for 40 min. For the electrochemical detection, the solution was transferred into an electrochemical cell containing 0.1 M HAc-NaAc buffer (pH=5.2) and OPD solution (0.8 mM). The differential pulse voltammetric measurements were performed from −0.1 to −0.8 V with pulse amplitude of 50 mV and a pulse width of 50 ms.

Results and discussion

Fabrication and characterization of the immunoelectrode

Since MWCNTs are chemically inert, activating their surface is an essential prerequisite for linking functional groups for anchoring CeO_2 mesoporous nanospheres. MWCNTs were initially oxidized by acid treatment to introduce carboxyl groups on their tips and any defect in the side walls. As demonstrated by previous report, PDDA was adsorbed on the surface of MWCNTs by electrostatic interaction between carboxyl groups on the MWCNTs surface and polyelectrolyte chains. Here, PDDA were assembled on MWCNTs at the activated GCE surface, then CeO_2 mesoporous nanospheres can be electrostatic absorbed on the MWCNTs surface. PSA antibodies were finally immobilizated onto the CeO_2 mesoporous nanospheres because of the strong interaction between the carboxyl groups on the CeO_2 mesoporous nanospheres and primary amine groups of antibodies. Finally, the BSA solution was used to block the residual active sites and reduce the nonspecific adsorption.

Scanning Electron microscopy (SEM) was employed to characterize the MWCNTs, PDDA functionalized MWCNTs, MWCNTs/PDDA/CeO_2 and MWCNTs/PDDA/CeO_2/Ab_1 assembled on GCE surfaces, respectively. As shown in Fig. 1a, the MWCNTs showed a well-dispersed one-dimensional structure and the diameter was in the range of 40-100 nm. No obvious change was observed for PDDA functionalized MWCNTs (Fig. 1b). As shown in Fig. 1c, the CeO_2 mesoporous nanospheres with diameter of about 50 nm were successfully adsorbed on the MWCNTs surface. From the image in Fig. 1d, PSA antibodies were immobilized onto the CeO_2 mesoporous nanospheres by the EDC and NHS crosslinking.

Impedance spectroscopy was reported as an effective method to monitor the feature of surface allowing the understanding of chemical transformation and processed associated with the conductive electrode surface [29]. The impedance spectra include a semicircle portion and a linear portion, the semicircle portion at higher frequencies corresponds to the electron-transfer limited process, and the linear part at lower frequencies corresponds to the diffusion process. The semicircle diameter corresponds to the electron transfer resistance (*R*et). Figure 2 shows the Nyquist plots of EIS for the bare GCE, (b) GCE/MWCNTs, (c) GCE/MWCNTs/PDDA, (d) GCE/MWCNTs/PDDA/CeO_2, (e) GCE/MWCNTs/PDDA/CeO_2/Ab_1, (f) GCE/MWCNTs/PDDA/CeO_2/Ab_1/Ag. At a bare GCE, the redox process of the $[Fe(CN)_6]^{3-/4-}$ probe showed an electron-transfer resistance of about 250 Ω (curve a in

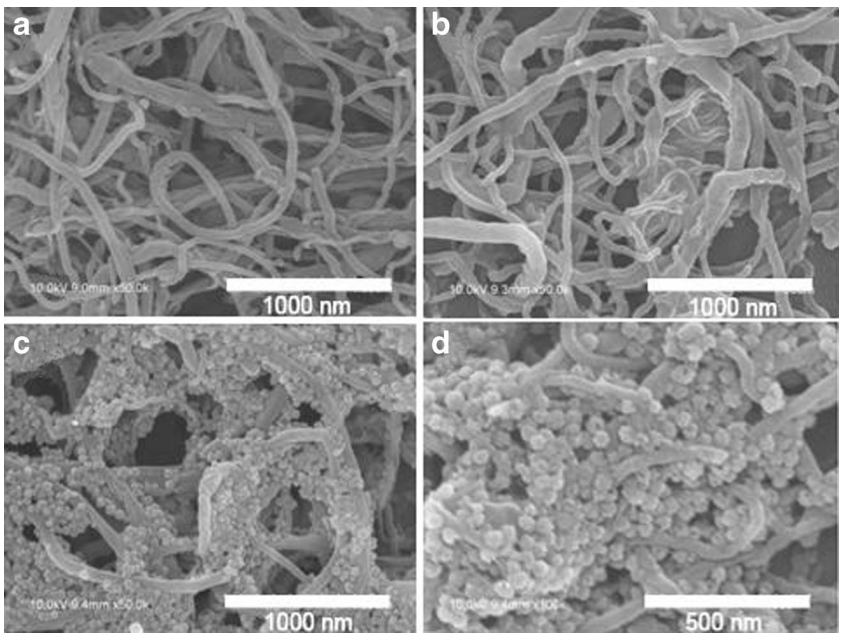

Fig. 1 SEM images of (**a**) GCE/MWCNTs, (**b**) GCE/MWCNTs/PDDA, (**c**) GCE/MWCNTs/PDDA/CeO_2, (**d**) GCE/MWNTs/PDDA/CeO_2/Ab_1

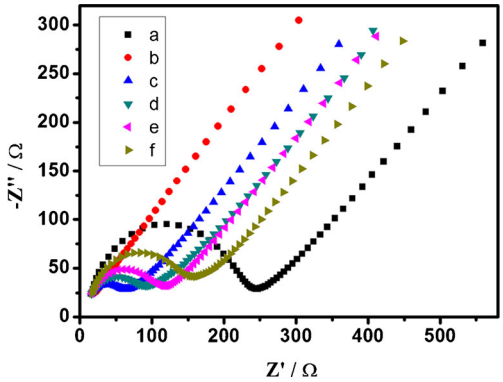

Fig. 2 Nyquist diagrams for the electrochemical impedance measurements in a solution of 0.1 M KNO_3 containing 5 mM $K_3Fe(CN)_6$ and 5 mM $K_4Fe(CN)_6$ for different electrodes (**a**) GCE, (**b**) GCE/MWCNTs, (**c**) GCE/MWCNTs/PDDA, (**d**) GCE/MWCNTs/PDDA/CeO_2, (**e**) GCE/MWCNTs/PDDA/CeO_2/Ab_1, (**f**) GCE/MWCNTs/PDDA/CeO_2/Ab_1/Ag

Fig. 2). The MWCNTs and MWCNTs/PDDA modified GCE both showed a much lower resistance for the redox probe (curves b, c in Fig. 2), implying that the MWCNTs and MWCNTs/PDDA were both an excellent electric conducting material and accelerated the electron transfer. After CeO_2 were assembled on the GCE/MWCNTs/PDDA, the electron-transfer resistance increased to 90 Ω (curve d in Fig. 2). When Ab_1 and PSA molecules were immobilized on the electrode (curve e and f in Fig. 2), the electron-transfer resistance increased, suggesting that the Ab_1 and PSA molecules can block the electron exchange between the redox probe and the electrode. The results were consistent with the observation from the SEM images as shown in Fig. 1.

Cyclic voltammetric behavior of the immunoelectrode

Figure 3 shows the cyclic voltammograms of different modified glassy carbon electrode in 0.1 M HAc-NaAc buffer solution (pH5.2) in the absence and presence of OPD. No amperometric response was observed at bare GCE, MWCNTs and MWCNTs/PDDA modified GCE in 0.1 M HAc-NaAc buffer solution (pH5.2) containing 0.8 mM OPD (curve a, b, c in Fig. 3). The above results indicated that the MWCNTs and PDDA could not have any catalytic effects on OPD oxidation. As shown in Fig. 3, curve g, no detectable current signal was observed for the MWCNTs/PDDA/CeO_2 modified GCE in the absence of OPD. This result showed that the CeO_2 itself had no electrochemical redox behavior in 0.1 M HAc-NaAc buffer solution (pH5.2). For the MWCNTs/PDDA/CeO_2 modified GCE in the presence of OPD (curve d in Fig. 3), a pair of stable redox peaks were observed at −0.47 V and −0.42 V (vs. SCE), respectively, corresponding to the redox 2,2-diaminoazobenzene, the oxidation product. Thus, the oxidation of OPD quickly went to the completion under the catalysis of CeO_2. The result confirmed that the CeO_2 mesoporous nanospheres had excellent catalytic property on the oxidation of OPD without any other oxidants. When the PSA antibodies and antigen were immobilized on the modified GCE (Fig. 3, curve e and f), the anodic peak current decreased obviously. It is reported that the activity of CeO_2 is dependent on the thickness of the polymer coating on the surface of cerium oxide nanoparticles [24]. Thus, the reason for the decreased current signals is that the antibody and antigen molecules covered on the CeO_2 mesoporous nanospheres, weakening the catalytic property of CeO_2. Therefore, a novel electrochemical immunoassay was developed for detection of PSA.

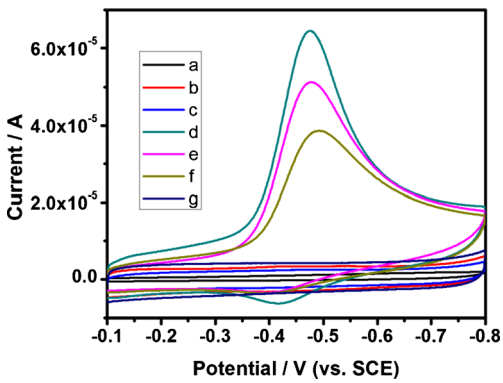

Fig. 3 Cyclic voltammograms of (**a**) glassy carbon electrode (GCE), (**b**) GCE/MWCNTs, (**c**) GCE/MWCNTs/PDDA, (**d**) GCE/MWCNTs/PDDA/CeO_2, (**e**) GCE/MWCNTs/PDDA/CeO_2/Ab_1, (**f**) GCE/MWCNTs/PDDA/CeO_2/Ab_1/Ag in 0.1 M HAc-NaAc buffer solution containing 0.8 mM OPD, (**g**) GCE/MWCNTs/PDDA/CeO_2 in 0.1 M HAc-NaAc buffer solution (pH5.2). SCE=saturated calomel electrode

Optimization of conditions for electrochemical detection of PSA

The analytical performance of the electrochemical detection was related to the concentration of CeO_2 and OPD in the measuring system. As seen in Fig. 4, the DPV peak current reached the similar maximum values at the CeO_2 and OPD concentrations of 0.5 mg mL^{-1} (Fig. 4a) and 0.8 mM (Fig. 4b), respectively. Therefore, the optimal concentrations of CeO_2 nanoparticles and OPD concentrations were selected at 0.5 mg mL^{-1} and 0.8 mM, respectively. Under optimal detection conditions, the electrochemical response depends on the formation of immunocomplex on the electrode surface. The latter is decided by the concentration of immobilized Ab_1 and the incubation time. In order to obtain the optimal concentration of Ab_1, the modified electrodes GCE/MWNTs/PDDA/CeO_2 were incubated in Ab_1 solutions with different concentrations. As shown in Fig. 4c, the peak currents increased with the increasing Ab_1 concentration and tended to a plateau at 40 μg mL^{-1}, indicating that immobilized Ab_1 reached a maximum absorption on the electrode. Thus, 40 μg mL^{-1} of Ab_1 was used for the immobilization. The effect of the antigen-antibody incubation time upon

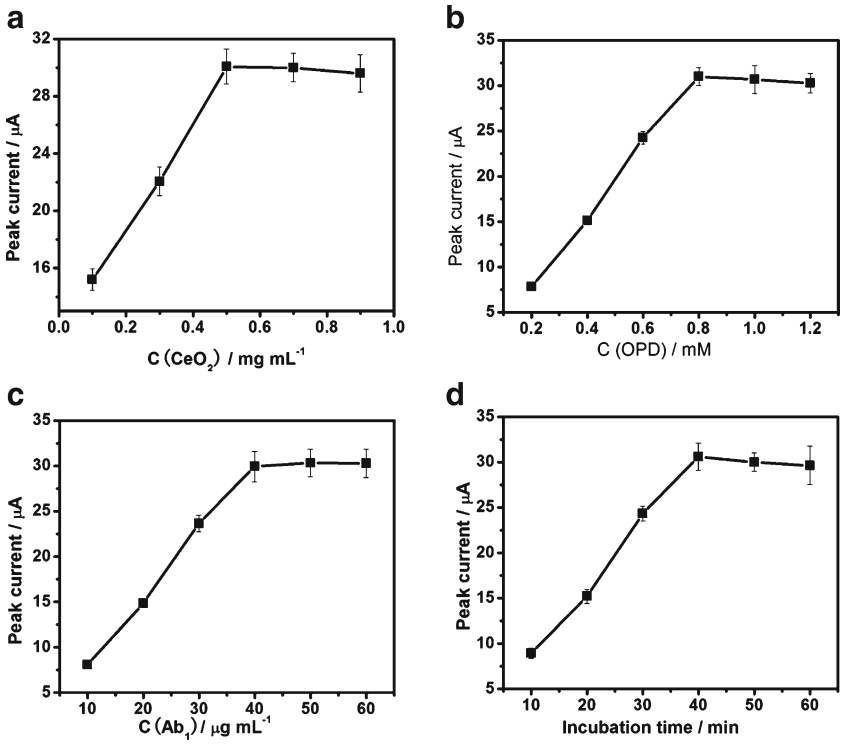

Fig. 4 Effects of (**a**) Concentration of CeO_2, (**b**) Concentration of OPD, (**c**) Concentration of PSA antibodies for immobilization, (**d**) Incubation time on current responses of PSA (10 pg mL^{-1}) in the assay

the peak current was shown in Fig. 4d. The response increased with the incubation time between 10 and 60 min and then leveled off after 40 min. The result indicated that the interaction of antigen with antibody had reached equilibrium after 40 min. therefore, to maximize the signal and minimize the assay time, 40 min was selected as the optimal incubation time.

Electrochemical response to PSA

It was found that the peak current of the DPV analysis decreased with the addition of PSA, as can be seen from Fig. 5a. The electrochemical PSA immunoassay displayed well-defined concentration dependence. As shown in Fig. 5b, a linear relation between the decreased peak current responses and the logarithmic values of antigen concentrations was observed in a range from 0.01 to 1,000 pg mL^{-1}. The linear regression equation was y=8.30 x +21.53 with a correlation coefficient R2=0.997 (n=6). The decreased peak current (ΔI) was calculated by the peak current differences for GCE/MWCNTs/CeO_2/Ab_1 and GCE/MWCNTs/CeO_2/Ab_1/Ag. As can be seen from Fig. 5b, ΔI increased with increasing PSA concentrations within the detection range. The detection limit of this immunoassay was 0.004 pg mL^{-1}. According to the linear equation, we could detect PSA concentration quantitatively. The analytical performance of the developed assay has

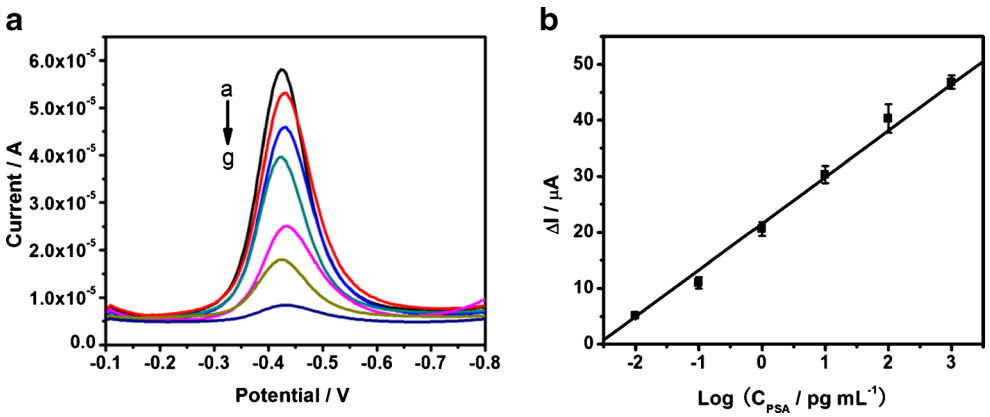

Fig. 5 **a** Typical differential pulse voltammetry of electrochemical immunoassay with increasing PSA concentration from (a) to (g) (0, 0.01, 0.1, 1.0, 10, 100, and 1,000 pg mL^{-1} PSA, respectively). **b** The resulting calibration curve of PSA plotted on a semi-log scale

Table 1 Performance comparison of different electrochemical methods

Method	Materials used	Linear range	Detection limit	Reference
Immunosensor	Carbon nanotubes	0.4–40 ng mL^{-1}	4 pg mL^{-1}	[30]
Aptasensor	gold nanoparticles encapsulated graphitized mesoporous carbon	0.25–200 ng mL^{-1}	0.25 ng mL^{-1}	[31]
Immunosensor	Nanoporous gold	0.05–26 ng mL^{-1}	3 pg mL^{-1}	[32]
Immunosensor	Graphene sheet	0.01–40 ng mL^{-1}	2 pg mL^{-1}	[33]
Immunosensor	liposome	0.01–100 ng mL^{-1}	7 pg mL^{-1}	[34]
Immunoassay	MWNTs/CeO2	0.01–1,000 pg mL^{-1}	0.004 pg mL^{-1}	This work

been compared with other detection methods in Table 1. It can be seen that the developed immunoassay showed a wider linear range and lower detection limit. This result may be attributed to the excellent catalytic property of CeO_2 for OPD and good conductivity of MWCNTs for electrochemical detection.

Specificity, reproducibility and stability of the PSA immunoassay

Specificity is an important criterion for analytical measurement. Other proteins such as α-fetoprotein (AFP), carcinoembryonic antigen (CEA) and human immunoglobulin G (HIgG) were used to evaluate the selectivity of the immunoassay. The current values obtained for each interfering substance at a concentration of 10 pg mL^{-1} was used as an indicator for the assay selectivity in comparison with the PSA reading alone. As could be seen in Fig. 6, no differences for interferences was observed, which indicated that the strategy had sufficient selectivity for PSA detection, and was capable of differentiating PSA from its analogues in complex samples. The intra-assay precision of the immunoassay was evaluated by assaying PSA at two levels for five replicate measurements. The intra-assay variation coefficients with this method were 3.1 % and 5.8 % at PSA concentrations of 1.0 pg mL^{-1} and 10 pg mL^{-1}, respectively, showing a good repeatability. While the interassay variation coefficients at these concentrations on five immunoassays made independently were 4.9 % and 6.1 %, respectively, indicating acceptable fabrication reproducibility. When the immunoelectrode was not in use, it was store at 4 °C. 95.8 % of the initial response of the immunoelectrode for PSA remained after two weeks, and 86.2 % of the initial response remained after four weeks. These results indicated the immunoelectrode had acceptable stability. The regeneration of the immunoelectrode could be realized by rinsing with pH 2.8 glycine-HCl solutions to dissociate the antigen-antibody complex. The as-renewed immunoelectrode could restore 90.2 % of the initial values after five assay runs, show accepted reusability.

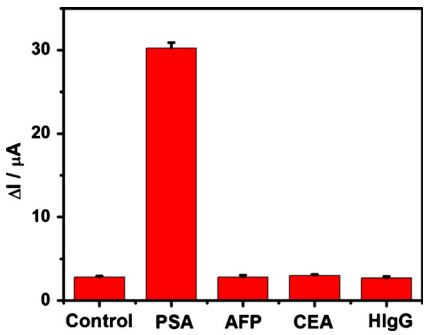

Fig. 6 The selectivity of the immunoassay. The concentration of antigen is 10 pg mL^{-1}. Error bars show the standard deviations of measurements taken from at least three independent experiments

Application of the immunoassay in human PSA levels

The feasibility of our developed immunoassay for clinical applications was investigated by analyzing real samples, in comparison with the enzyme linked immunosorbent assay (ELISA) method. Table 2 described the correlation between the partial results obtained by the immunoassay and the ELISA method. It obviously indicated that there was no significant difference between the results given by the two methods, which meant that the immunoassay could be satisfactorily applied to the clinical determination of PSA levels in human plasma.

Table 2 Assay results of clinical serum samples using the and ELISA methods

Serum Samples	Our method[a] (ng mL^{-1})	ELISA[a] (ng mL^{-1})	Relative deviation (%)
1	1.20	1.26	−4.8
2	0.60	0.57	5.2
3	102.2	101.3	0.9
4	27.50	27.94	−1.6
5	15.62	15.90	−0.8

[a] The average value of five successive determinations

Conclusion

A sensitive electrochemical immunoassay was developed for PSA detection based on the catalytic property of CeO_2 mesoporous nanospheres to OPD oxidation. The designed immunoassay for PSA had good performance with high sensitivity, a wide linear range, acceptable precision and fabrication reproducibility, and excellent stability. It had been successfully applied in the detection of PSA in serum samples. The immobilization strategy provides a useful platform for electrochemical immunoassay for wide-range cancer biomarkers and could be readily extended toward the on-site monitoring of the cancer biomarkers in serum samples.

Acknowledgements We greatly appreciate the support of the National Natural Science Foundation of China (Nos: 21265014, 21121091, 21075061, 21103088) and Program for New Century Excellent Talents in University (NCET-12-0256). This work is also supported by Research Starting Funds for Imported Talents (BQD2012010), Ningxia University. The authors extend their appreciation to the Deanship of Scientific Research at King Saud University for funding the work through the research group project (RGP-VPP-029).

References

1. Ludwig JA, Weinstein JN (2005) Biomarkers in cancer staging, prognosis and treatment selection. Nat Rev Cancer 5:845–856
2. Gubala V, Harris LF, Ricco AJ, Tan MX, Williams DE (2012) Point of care diagnostics: status and future. Anal Chem 84:487–515
3. Lai GS, Yan F, Ju HX (2009) Dual Signal amplification of glucose oxidase-functionalized nanocomposites as a trace label for ultrasensitive simultaneous multiplexed electrochemical detection of tumor markers. Anal Chem 81:9730–9736
4. Kreisig T, Hoffmann R, Zuchner T (2011) Homogeneous fluorescence-based immunoassay detecs antigens within 90 seconds. Anal Chem 83:4281–4287
5. Xu SJ, Liu Y, Wang TH, Li JH (2001) Positive potential operation of a cathodic electrogenerated chemiluminescence immunosensor based on luminol and graphene for cancer biomarker detection. Anal Chem 83:3817–3823
6. Wang Y, Dostalek J, Knoll W (2011) Magnetic nanoparticle-enhanced biosensor based on grating-coupled surface plasmon resonance. Anal Chem 83:6202–6207
7. Yang Y, Zhu YC, Chen Q, Liu YY, Zeng Y, Xu FF (2009) Carbon-nanotube-activated Pt quart-crystal microbalance for the immunoassay of Human IgG. Small 5:351–355
8. Tang DP, Yuan R, Chai YQ (2008) Quartz crystal microbalance immunoassay for carcinoma antigen 125 based on gold nanowire-functionalized biomimetic interface. Analyst 133:933–938
9. Kimmel DW, LeBlanc G, Meschievitz ME, Cliffel DE (2012) Electrochemical Sensors and Biosensors. Anal Chem 84:685–707
10. Du D, Zou ZX, Shin YS, Wang J, Wu H, Engelhard MH, Liu J, Aksay IA, Lin YH (2010) Sensitive immunosensor for cancer biomarker based on dual signal amplification strategy of graphene sheets and multienzyme functionalized carbon nanospheres. Anal Chem 82: 2989–2995
11. Zhuo Y, Yuan R, Chai YQ, Tang DP, Zhang Y, Wang N, Li XL, Zhu Q (2005) A reagentless amperometric immunosensor based on gold nanoparticles/thionine/Nafion-membrane-modified gold electrode for determination of alpha-1-fetoprotein. Electrochem Commun 7: 355–360
12. Alivisatos P (2004) The use of nanocrystals in biological detection. Nat Biotechnol 22:47–52
13. Rosi NL, Mirkin CA (2005) Nanostructures in biodiagnostics. Chem Rev 105:1547–1562
14. Katz E, Willner I (2004) Integrated nanoparticle-biomolecule hybrid systems: Synthesis, properties, and applications. Angew Chem Int Ed 43:6042–6108
15. Astruc D, Lu F, Aranzaes JR (2005) Nanoparticles as recyclable catalysts: The frontier between homogeneous and heterogeneous catalysis. Angew Chem Int Ed 44:7852–7872
16. Raimondi F, Scherer GG, Kotz R, Wokaun A (2005) Nanoparticles in energy technology: Examples from electrochemistry and catalysis. Angew Chem Int Ed 44:2190–2209
17. Choi JH, Nguyen FT, Barone PW, Heller DA, Moll AE, Patel D, Boppart SA, Strano MS (2007) Multimodal biomedical imaging with asymmetric single-walled carbon nanotube/iron oxide nanoparticle complexes. Nano Lett 7:861–867
18. Trovarelli A (1996) Catalytic properties of ceria and CeO_2-containing materials. Catal Rev Sci Eng 38:439–459
19. Kaspar J, Fornasiero P, Graziani M (1999) Use of CeO_2-based oxides in the three way catalysis. Catal Today 50:285–298
20. Rodriguez JA, Hanson JC, Kim JY, Liu G, Iglesias-Juez A, Fernandez-Garcia M (2003) Properties of CeO_2 and $Ce_{1-x}Zr_xO_2$ nanoparticles: X-ray absorption near-edge spectroscopy, density functional, and time-resolved x-ray diffraction studies. J Phys Chem B107:3535–3547
21. Zhou KB, Wang X, Sun XM, Peng Q, Li YD (2005) Enhanced catalytic activity of ceria nanorods from well-defined reactive crystal planes. J Catal 229:206–212
22. Guzman J, Carrettin S, Corma A (2005) Spectroscopic evidence for the supply of reactive oxygen during CO oxidation catalyzed by gold supported on nanocrystalline CeO_2. J Am Chem Soc 127:3286–3287
23. Carrettin S, Concepcion P, Corma A, Nieto JML, Puntes VF (2004) Nanocrystalline CeO_2 increases the activity for CO oxidation by two orders of magnitude. Angew Chem Int Ed 43:2538–2540
24. Asati A, Santra S, Kaittanis C, Nath S, Perez JM (2009) Oxidase-like activity of polymer-coated cerium oxide nanoparticles. Angew Chem Int Ed 48:2308–2312
25. Asati A, Santra S, Kaittanis C, Nath S, Perez JM (2011) pH-tunable oxidase-like activity of cerium oxide nanoparticles achieving sensitive fluorigenic detection of cancer biomarkers at neutral pH. Anal Chem 83:2547–2553
26. Gao RF, Zheng JB, Zheng XZ (2011) Direct electrochemistry of myoglobin in a layer-by-layer film on an ionic liquid modified electrode containing CeO2 nanoparticles and hyaluronic acid. Microchim Acta 174:273–280
27. Qiu JD, Cui SG, Liang RP (2010) Hydrogen peroxide biosensor based on the direct electrochemistry of myoglobin immobilized on ceria nanoparticles coated with multiwalled carbon nanotubes by a hydrothermal synthetic method. Microchim Acta 171:333–339
28. Liang X, Xiao JJ, Chen BH, Li YD (2010) Catalytically stable and active CeO_2 mesoporous spheres. Inorg Chem 49:8188–8190
29. Bard AJ, Faulkner LR (1980) Electrochemical Methods. Wiley, New York
30. Yu X, Munge B, Patel V, Jensen G, Bhirde A, Gong JD, Kim SN, Gilespie J, Gutkind JS, Papadimitrakopoulous F, Rusling JF Carbon nanotube amplification strategies for highly sensitive immunodetection of cancer biomarkers. J Am Chem Soc 128: 11199–11205
31. Liu B, Lu LS, Hua EH, Jiang ST, Xie GM (2012) Detection of the human prostate-specific antigen using an aptasensor with gold nanoparticles encapsulated by graphitized mesoporous carbon. Microchim Acta 178:163–170

32. Wei Q, Zhao YF, Xu CX, Wu D, Cai YY, He J, Li H, Du B, Yang MH (2011) Nanoporous gold film based immunosensor for label-free detection of cancer biomarker. Biosens Bioelectron 26:3714–3718
33. Li H, Wei Q, He J, Li T, Zhao YF, Cai YY, Du B, Qian ZY, Yang MH (2011) Electrochemical immunosensors for cancer biomarker with signal amplification based on ferrocene functionalized iron oxide nanoparticles. Biosens Bioelectron 26:3590–3595
34. Qu B, Guo L, Chu X, Wu DH, Shen GL, Yu RQ (2010) An electrochemical immunosensor based on enzyme-encapsulated liposomes and biocatalytic metal deposition. Anal Chim Acta 663:147–152